J Mater Sci: Mater Med (2010) 21:431–438
DOI 10.1007/s10856-009-3890-2

Injectability of brushite-forming Mg-substituted and Sr-substituted α-TCP bone cements

S. Pina · P. M. C. Torres · J. M. F. Ferreira

Received: 16 June 2009 / Accepted: 1 October 2009 / Published online: 23 October 2009

Abstract The influence of magnesium- and strontium-substitutions on injectability and mechanical performance of brushite-forming α-TCP cements has been evaluated in the present work. The effects of Mg- and Sr-substitutions on crystalline phase composition and lattice parameters were determined through quantitative X-ray phase analysis and structural Rietveld refinement of the starting calcium phosphate powders and of the hardened cements. A noticeable dependence of injectability on the liquid-to-powder ratio (LPR), smooth plots of extrusion force versus syringe plunger displacement and the absence of filter pressing effects were observed. For LPR values up to 0.36 ml g^{-1}, the percentage of injectability was always higher and lower for Mg-containing cements and for Sr-containing cements, respectively, while all the pastes could be fully injected for LPR $>$ 0.36 ml g^{-1}. The hardened cements exhibited relatively high wet compressive strength values ($\sim$17–25 MPa) being the Sr- and Mg-containing cements the strongest and the weakest, respectively, holding an interesting promise for uses in trauma surgery such as for filling bone defects and in minimally invasive techniques such as percutaneous vertebroplasty to fill lesions and strengthen the osteoporotic bone.

1 Introduction

The continued increase in the age of population and the concomitant increasing incidence of bone diseases such osteoporosis (a disease that results in a loss of normal bone density, mass and strength, leading to a condition in which bones are increasingly porous or full of small holes and vulnerable to breaking), osteomyelitis, malignant tumors, or traumatic accidents, has generated higher demands for bone grafting [1, 2]. Vertebroplasty and kyphoplasty are minimally invasive procedures for vertebral compression fractures (VCF) usually caused by osteoporosis, which are fractures in vertebra, the small bones that make up the spinal column.

The orthopedic cements used in vertebroplasty and kyphoplasty are based on polymethylmethacrylate (PMMA) for their satisfactory mechanical properties. However, this kind of cements might cause extensive necrosis due to noticeable exothermal effects upon curing [2–5]. Besides, PMMA cements have several other drawbacks, including no biologic potential to remodel or integrate into the surrounding bone, no direct bone apposition, excessive inherent stiffness, high polymerization temperature, and potential monomer toxicity. PMMA is also commonly used as bone void filler in surgery requiring the removal of bone as in bone tumours [6, 7].

Calcium phosphate cements (CPC) have been in clinical use for the last 10 years. They are prepared from a powder and a liquid, forming a viscous and easy mouldable paste that after being implanted sets and hardens within the body as either a non-stoichiometric calcium deficient hydroxyapatite (CDHA) or brushite, sometimes blended with unreacted particles and other phases. They are commonly used as bone filling defects and in trauma surgeries as mouldable paste-like bone substitute materials. Their most salient features include good biocompatibility, excellent bioactivity, self-setting characteristic, low setting temperature, adequate stiffness, and easy shaping to any complicated geometry [8–16]. Nearly perfect adaptation to tissue surfaces in bone defects, a gradual bioresorption followed

S. Pina (✉) · P. M. C. Torres · J. M. F. Ferreira
Department of Ceramics and Glass Engineering, University of Aveiro, CICECO, 3810-193 Aveiro, Portugal
e-mail: sandra.pina@ua.pt

by new bone formation and the lack of any by-products are other distinctive advantages of CPC [6, 7].

Recently, the development of injectable CPC is seen with alacrity due to their importance for minimally invasive surgical techniques such as percutaneous vertebroplasty to fill bone lesions and cracks to strengthen the bone [15, 17–22]. Injectable osteoconductive CPC can fit bone defects perfectly and be used as an adjunct to internal fixation for treating selected fractures, as filling voids in metaphyseal bone, thereby reducing the need for bone graft, and improving the holding strength around metal devices in osteoporotic bone. They can easily be used by bone remodeling cells for reconstruction of damaged parts of bones [11, 15]. Injectability is also important for applications with limited accessibility and narrow cavities, and when there is a need for precise placement of the paste to conform to a defect area, such as periodontal bone repair and tooth root canal fillings. However, liquid-phase separation (the so-called filter-pressing effect) provoked by the extrusion pressure applied to the cement paste after a certain injection time has often been observed in commercial formulations [4, 23]. This problem has been the focus of several previous studies [4, 11, 15, 21–26]. Habib et al. [23] concluded that high extrusion velocity, small syringe size, short cannula and high liquid-to-powder ratio (LPR) favoured injectability. Sarda et al. [21] found enhanced injectability of α-TCP-water mixtures with the addition of citrate ions. Barralet et al. [24] made similar observations for brushite and apatite cements and found improved injectability with increasing LPR. Leroux et al. [26] used sodium glycerophosphate, latic acid, glycerol and chitosan to improve injectability and measured lower extrusion forces in the presence of all these additives. However, commercial formulations still suffer from several shortcomings related to unsatisfactory levels of some properties: (i) low mechanical strength; (ii) poor injectability; (iii) ionic mismatches towards the bone composition, which includes (but is not limited to) the following cations: Na^+, K^+, Mg^{2+}, Ca^{2+}, H^+ and anions: PO_4^{3-}, HPO_4^{2-}, $H_2PO_4^-$, CO_3^{2-}, HCO_3^-, SO_4^{2-}, HSO_4^-, Cl^-, F^-, SiO_4^{4-} [4, 7, 11, 15]. Insufficient mechanical strength and the poor injectability are interdependent properties, both affected by a number of experimental factors, such as particle size and particle size distribution of the powder, the degree of crystallinity (amorphous calcium phosphates tend to give more viscous and reactive mixtures), the presence of rheological modifiers and/or other additives with specific roles. Usually, injectability of a cement paste varies inversely with its viscosity and with the time after starting the mixing of liquid and powder [4, 7, 23, 26]. Enhancing the injectability of a cement paste by increasing LPR degrades the mechanical properties and cohesion of hardened cements and markedly elongates the initial and final setting times [7].

Substitution of trace elements, such as Mg and Sr ions in the apatite structure has been the subject of widespread investigation, because of their impending role in the biological process, as observed during implantation studies [27–35]. Mg is undoubtedly one of the most important bivalent ions associated with the biological apatite; Sr increases osteoclast apoptosis and enhances preosteoblastic cell proliferation and collagen synthesis [35]. However, none of the above mentioned literature reports have been focused on studying the injectability of brushite-forming Mg- and Sr-substituted α-TCP cements. Therefore, the main goal of the present study is to investigate the influence of single Mg- and Sr-substitutions on the injectability of brushite-forming α-TCP cements.

2 Materials and methods

2.1 Preparation of powders and cement pastes

The Mg- and Sr-substituted cements with molar ratio (Ca + x)/P = (1.35 + 0.15)/1 = 1.5 (x denoting the molar content of Sr or Mg), thus performing the stoichiometric ratio of β-TCP, were used in the present study. The starting Mg- and Sr-substituted powders were prepared by aqueous precipitation as described elsewhere [36]. Briefly, calcium nitrate tetrahydrate [$Ca(NO_3)\cdot 4H_2O$, Vaz Pereira-Portugal, Sintra, Portugal], diammonium hydrogen phosphate [$(NH_4)_2HPO_4$, Vaz Pereira-Portugal, Sintra, Portugal], magnesium nitrate hexahydrate [$Mg(NO_3)_2\cdot 6H_2O$, Merck, Darmstadt, Germany] and strontium nitrate [$Sr(NO_3)$, Riedel-de-Haen, Seelze, Germany] were used as starting chemical precursors, respectively for calcium, phosphorous, magnesium and strontium. The precipitates were filtrated, dried at 110°C and then heat treated at 1500°C to convert them mostly into α-TCP.

The calcined cakes were milled and passed through a 36 μm sieve and then used as starting CPC powders. Particle size distributions of the powders were determined using a light scattering instrument (Coulter LS 230, UK, Fraunhofer optical model). The particle morphology of the powders was obtained using a scanning electron microscope (SEM) (Hitachi S4100, Tokyo, Japan).

Cement pastes were prepared by mixing different proportions of the starting CPC powders with an aqueous solution consisting of 20 wt% citric acid (Sigma) + 10 wt% poly(ethylene glycol) (PEG) (200, Sigma) + 0.5 wt% hydroxyl propyl methylcellulose (HPMC) (3.5–5.6 mPa s at 2% by mass in water, Sigma) in order to get liquid-to-powder ratios (LPR) of 0.34, 0.35, 0.36 and 0.38 ml g^{-1}.

These cements will be hereafter designated as Mg-BC and Sr-BC, respectively for Mg- and Sr-substituted cements. For comparison purposes and a better understanding of the effects of Mg and Sr on injectability of substituted cement pastes, pure α-TCP cement was also prepared and used as reference (Ref-BC).

2.2 X-ray diffraction and structural analysis by the Rietveld refinement method

Identification of the crystalline phases formed upon hydration of cement pastes was performed by X-ray diffraction (XRD) using a high-resolution SIEMENS D5000 with SolX detector. Data sets were collected from $2\theta = 10$–$50°$ with a step size of 0.02°, with CuKα radiation. The phase composition of the samples was calculated on the basis of XRD patterns by means of Rietveld analysis with TOPAS 3.0 software (Bruker AXS, Germany). Rietveld refinement was performed using the structural models (ICSD Database) of all phases listed in Table 1.

2.3 Rheological measurements

Rheological measurements of the cement pastes were carried out with a rotational controlled-stress rheometer (Bohlin C-VOR 150, Bohlin Ltd., Gloucestershire, UK) equipped with a 4°/40 mm cone-and-plate sensor system. Viscosity measurements were performed in the shear rates range of about 0.1–100 s^{-1}. For each test, 2 g of powder was mixed with the setting liquid at LPR = 0.35 ml g^{-1}, for 1 min to form a homogeneous paste at room temperature. The rheological measurement started 1 min after mixing in order to assure the same rheological history during the preparation of all the cement pastes.

2.4 Setting times

The initial setting time of the cement pastes was determined using Vicat needle technique according to the ASTM C 187-98. One minute after placing the pastes into a glass plate stored at 37°C in 100% humidity box, the indenter (100 g in mass, 1 mm diameter of the needle) was lowered vertically onto the surface of the cement. The indentation was repeated at intervals of 30 s until no more penetration was possible. The time at this point was taken as the initial setting time.

Table 1 ICSD-Data used for Rietveld refinement and phase quantification

Phase	Structural model	
	ICSD code	Authors
α-TCP (tricalcium phosphate)	923	Mathew et al. [37]
β-TCP	97500	Yashima et al. [38]
Brushite (DCPD)	16132	Curry and Jones [39]

2.5 Injectability testing

The injectability tests were carried out with a 10 ml syringe (15 mm diameter and 80 mm in length) fitted with a cannula of 2.2 mm inner diameter and 91 mm in length, according to a procedure described in previous studies [9, 14, 40]. The paste (5 g of powder + the required amount of liquid) was hand-mixed for 1 min and then placed into the syringe. The syringe was placed between the compression plates of a testing machine (Shimadzu Autograph, Trapezium 2, Japan) using a home made apparatus fixture. The cement pastes were extruded at a crosshead speed of 15 mm min^{-1} up to a maximum load of 100 N. The evolution of the extrusion force was recorded against the extruding time and the percentage of extruded paste was determined as the mass of the paste that could be expelled from the syringe divided by the original mass of the paste inside the syringe [14, 40]. For each experimental set of conditions, injectability measurements were repeated three times and the average values calculated.

In order to evaluate the eventual occurrence of filter-pressing effects whenever the pastes could not be totally extruded, both the extruded pastes and the pastes remaining in the syringe were examined for the LPR. For that, the weights of the pastes before and after complete drying at 120°C for 24 h were measured.

2.6 Mechanical testing

Cement pastes were cast into PTFE-moulds (Φ 6 × 12 mm deep) and stored for 24 h in a 100% humidity box at 37°C. The cement specimens were then removed from the moulds and immersed in PBS solution at 37°C for additional 6, 24 and 48 h. The compressive strength measurements were done using a universal materials testing machine (Shimadzu Autograph, Trapezium 2, Japan) at a crosshead displacement rate of 1 mm min^{-1}. Results of compressive strength are expressed as the mean ± standard error of the mean of triplicate determinations.

2.7 Statistical analysis

Statistical analysis of injectability and mechanical strength data was performed using the SPSS 16.0 software. Comparative studies of means were performed using one-way ANOVA followed by a post hoc test (Fisher projected least-significant difference) with a statistical confidence coefficient of 95%; therefore, P-values < 0.05 were considered significant.

3 Results

Particle diameter distributions of the starting CPC powders after milling and sieving are depicted in Fig. 1. All size distribution curves are essentially monomodal with average particle diameters, D_{50}, of 17.32, 10.78, 15.97 μm, for Ref-BC, Sr-BC and Mg-BC powders, respectively. Minor populations centred at about 2 μm are also apparent, being somewhat more intense in the case of Sr-BC powder.

Figure 2 presents the XRD diffraction patterns of the powdered hardened undoped and Mg- or Sr-substituted cements after 2 days of hydration. All the hydrated cements consist mostly of α-TCP, and brushite as a minor crystalline phase. The presence of β-TCP is noted only in the case of Mg-substituted cement.

Quantitative Rietveld XRD analyses of phases on the starting powders and formed upon hydration for 2 days are presented in Table 2. The reported data confirm that the starting powders are mostly constituted by α-TCP for Ref-BC and Sr-BC cements, while for Mg-BC it consists of a mixture of α-TCP as the main phase and β-TCP as minor phase. The hydrated cements consist predominantly of α-TCP and a fraction of brushite, with an additional β-TCP phase in the case of Mg-BC.

The flow curves of the cement pastes with a LPR = 0.35 are presented in Fig. 3. All of them exhibit similar shear-thinning character. Although very close to each other, if ordered by decreasing viscosity at given shear rates, the curves appear as Sr-BC > Ref-BC > Mg-BC. Accordingly, the initial setting times of the cement pastes tended to increase in the same order: 5 ± 0.5 min for Ref-BC, 7 ± 0.5 min for Sr-BC and 10.0 ± 0.5 min for Mg-BC ($P < 0.05$).

The forces required for extruding the pastes as a function of syringe plunger displacement are shown in Fig. 4

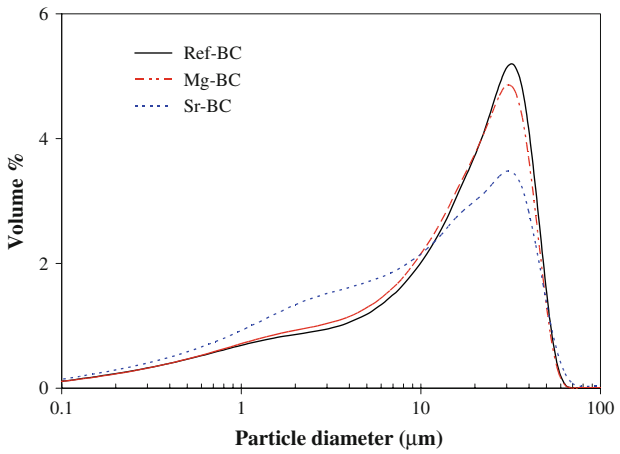

Fig. 1 Particle size distributions of the starting CPC powders after milling

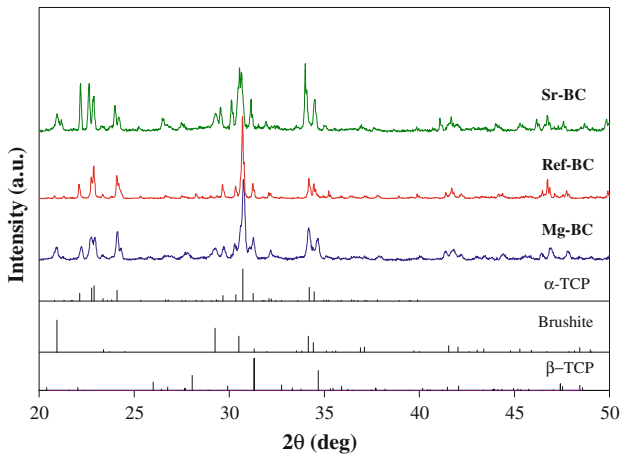

Fig. 2 XRD patterns of cements prepared from a mixing liquid with 0.5 wt% HPMC + 10 wt% PEG + 20 wt% citric acid, after 2 days of hydration. α-TCP ($Ca_3(PO_4)_2$, JCPDS PDF File # 29-359), Brushite (JCPDS PDF File # 9-0077) and β-TCP (β-$Ca_3(PO_4)_2$, JCPDS PDF File # 1-70-682); full scale intensity = 6000 cps

Table 2 Rietveld refinement phase analysis of the starting powders and of the cements hydrated for 2 days

Phases	Composition (%)					
	Ref-BC		Sr-BC		Mg-BC	
	Powder	Hydrated	Powder	Hydrated	Powder	Hydrated
α-TCP	100.0	77.5	100.0	77.3	84.6	71.8
Brushite	–	22.5	–	22.7	–	22.8
β-TCP	–	–	–	–	15.4	5.4

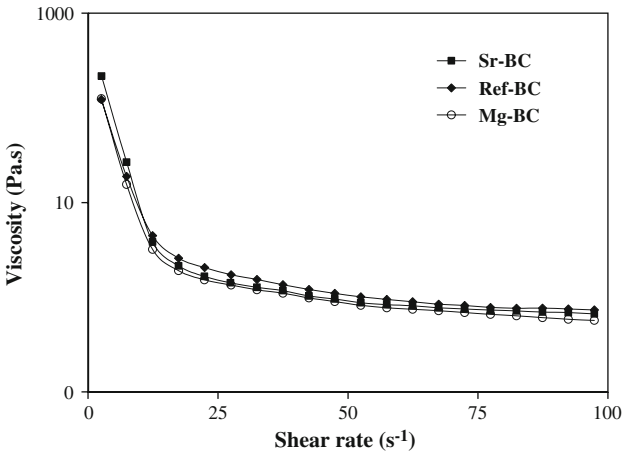

Fig. 3 Viscosity versus shear rate curves of the cement pastes prepared with LPR of 0.35 ml g^{-1}

for two different LPR values of 0.34 and 0.38 ml g^{-1}. It can be seen that for LPR = 0.34 ml g^{-1} the extrusion force soon exceeded the pre-set maximum force after 4.3–5.1 mm of plunger travel. The higher extrusion forces

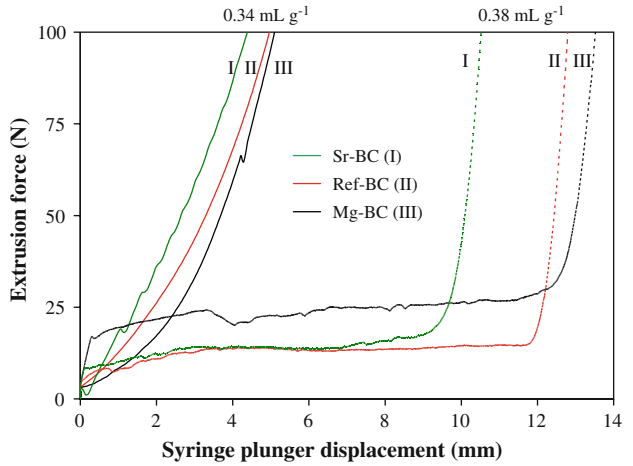

Fig. 4 Extrusion force versus syringe plunger displacement for cement pastes prepared with LPR of 0.35 ml g^{-1} (*continuous lines*) and of 0.38 ml g^{-1} (*dashed lines*)

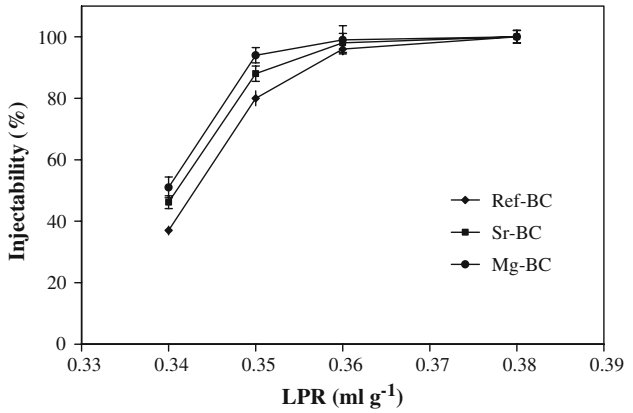

Fig. 5 Injectability of the cement pastes as function of LPR, 1.5 min after starting mixing the powder with the setting liquid

demanded for the lower LPR hindered full injection under the set conditions, although higher extrusion forces could be exerted even by hand injection. For the LPR = 0.38 ml g^{-1}, the extrusion curves present a relatively long plateau followed by a fast increase. The observed trends denote different reactivities of the starting cement powders ($P < 0.05$) towards the setting liquid. None of the cements presented the filter-pressing effect during extrusion from the syringe.

Figure 5 plots the dependence of the injectability of the cement pastes versus LPR in the range 0.34–0.38 ml g^{-1}, 1.5 min after starting mixing the powder with the setting liquid. It can be seen that the injectability increased with increasing LPR, due to the concomitant decrease of the viscosity of the pastes. Nearly full injectable pastes were obtained for LPR $\geq$ 0.38 ml g^{-1}. It is also observed that the composition of the starting powders influences the injectability. Mg-BC is the easiest injectable composition,

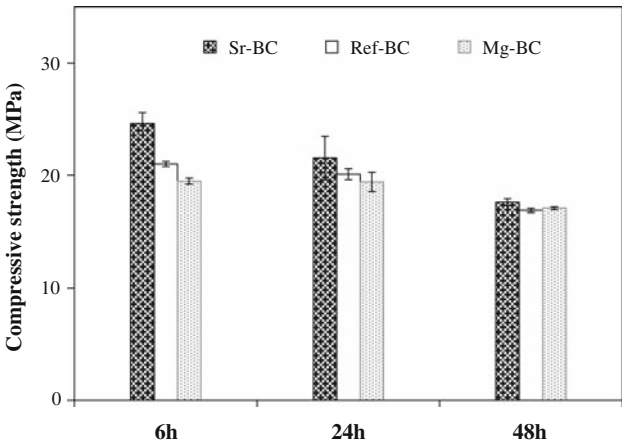

Fig. 6 Compressive strength values measured for the wet cements hydrated for 24 h and kept under wet conditions for further 6, 24 and 48 h. The pastes were prepared with 0.5 wt% HPMC + 10 wt% PEG + 20 wt% citric acid (LPR = 0.38 ml g^{-1})

probably due to the presence of some remaining β-TCP phase, which has a much longer handling time, and to the specific role of Mg in delaying the setting process [36].

The wet compressive strength values of the cements hardened for 24 h and kept under wet conditions for further 6, 24 and 48 h, before performing the measurements, are shown in Fig. 6. As expected, the compressive strength decreased with an increase of immersion time in PBS solution, due to a gradual structural degradation process ($P < 0.05$). It can be observed that Sr-BC cement specimens exhibit the highest compressive strength values, followed by Ref-BC cements ($P \cong 0.009$), and by Mg-BC cements ($P \cong 0.012$). This can be probably due to the presence of β-TCP phase in Mg-BC.

4 Discussion

Improving the less performing aspects of CPCs requires lowering the LPR values while keeping suitable flow properties. These requirements are not easy to conciliate, especially in reacting systems as cement pastes are. It has been shown that in non-reacting aqueous systems low viscosity suspensions of calcium phosphate powders containing unusual high solids loading (60 vol.%) could be easily prepared [41]. This solids loading corresponds to a LPR of 0.21 ml g^{-1}, much lower than those used in injectable CPC [7]. Therefore, the key to formulate strong injectable CPC is to decrease LPR while keeping a relatively low viscosity. This strategy to enhance the mechanical properties leads to a decrease of the cement porosity, which in turn will reduce the resorption kinetics. But this drawback can be coped using brushite-based CPC like the ones proposed in the present work, which have a faster resorption than apatite CPC [4, 36, 42]. Injectability

of CPC pastes is strongly dependent on their flow properties, which, in turn, depend on a number of factors including particle/agglomerate size and particle/agglomerate size distributions, the nature of the phases present (amorphous or crystalline), the liquid-to-powder ratio (LPR), and the presence of rheological modifiers. Injectability, the ability of the cement pastes to be extruded through relatively fine nozzles, requires a shear thinning behaviour. The presence of particle agglomerates with an open structure and sweeping large areas when the system flows tends to confer a shear thickening behaviour to the cement pastes, which, in turn, is the direct cause of the filter-pressing effect often observed in CPC pastes. Considering that the time allowed for mixing the starting CPC powders and setting liquid is short and that hand mixing is unsuitable for destroying particle agglomerates, it is essential that the starting powders have been already deagglomerated and possess a relatively wide particle size distribution [43]. This was the reason why the powders were milled/deagglomerated and passed through a 36 μm sieve before being used to prepare the cement pastes. This procedure, and probably the use of HPMC as gelling agent, fully prevented the filter-pressing phenomenon during extrusion from the syringe for all cement pastes.

The shear-thinning character revealed in Fig. 3 (LPR = 0.35) was typical of cement pastes with other LPR values. This type of rheological behaviour with viscosity decreasing as shear rate increases is very suitable for injection through narrow nozzles.

In order to check if the shear rate range adopted could well represent the injectability conditions, the maximum shear rate, τ_w, at the cannula wall was estimated based on the Hagen-Poiseuille equation for steady laminar flow [44]. The following holds for the maximum shear rate τ_w at the pipe wall:

$$\tau_w = \frac{4\dot{V}}{\pi R^3}$$

where $\dot{V}$ is the volume flow rate [$m^3\ s^{-1}$], and R is the inside diameter of the capillary [m]. The conditions set for injectability tests correspond to a volume flow rate of about 44.2×10^{-9} $m^3\ s^{-1}$ and a maximum shear rate at the inner cannula wall of about 16.6 s^{-1}. Therefore, the shear rate range used to access the flow behaviour covers all the possible values for this inner diameter (2.2 mm) of the cannula even if the volume flow rate was increased by six times.

The plots of extrusion force as a function of syringe plunger displacement shown in Fig. 4 reveal the dependence of extrusion force on the LPR as shown by several previous studies [4, 7, 21, 23, 26]. It is worthy noting that all the extrusion curves presented in Fig. 4 are smoother that those reported for similar LPR values but non-reacting systems. Such roughness was probably due to the presence of particles agglomerates, although their destruction would be easier in a non-reacting system [14].

Concerning the effects of ionic substitutions, the sets of extrusion curves presented in Fig. 4 show the same order: the Sr-BC is always shortest and the Mg-BC is the longest. This means that Sr enhances the reactivity of the cement pastes, while Mg tends to delay the setting process of α-TCP based cements. The remaining β-TCP phase in the starting powder of this cement, which has a much longer handling time is also expected to improve the injectability. This is according to what has been reported earlier for the influence of Sr-substituted and Mg-substituted cements [35, 45]. Lilley et al. [34] showed a strong effect of Mg on setting kinetics and on the characteristics of hardened cements namely, a decreasing rate of hydration, an increased proportion of brushite formed upon setting, and a decrease in compressive strength. Mg has been also reported to have a stabilizing role of non-crystalline CaPs, preventing crystallization into other more stable CaP phases [46], in good agreement with an observed decrease of the hydrolysis extent of brushite [34]. Bone restoration studies made in rats showed that using CPC doped with low doses of Sr increased the number of bone forming sites and vertebral bone volume, while no adverse effects could be observed on mineral profile, bone mineral chemistry or bone matrix mineralization [47]. Saint-Jean et al. [48] reported comparable bioactivities for hardened Sr-containing apatite cements and calcium deficient hydroxyapatite.

The injectability results plotted in Fig. 5 are in good agreement with the extrusion curves shown in Fig. 4 and with data reported in previous studies [49]. For LPR values up to 0.36 ml g^{-1}, the percentage of injectability is always higher for the case of Mg-BC and lower for Sr-BC. For LPR > 0.36 ml g^{-1} all the pastes could be fully injected under the relatively low applied forces set in the present work.

The measured wet compressive strength values (~17–25 MPa) of the cements are in the upper limit of range of 1–25 MPa for compressive strengths reported in literature for brushite-forming cements [6] as well as in the range for cancellous bone (10–30 MPa) [50]. The results show that Sr-containing cement specimens exhibit higher compressive strength values in comparison to undoped Ref-BC followed by Mg-BC cement, probably due to the lower content of brushite phase present in Sr-BC (pure brushite cements are characterized by their low mechanical strength). Citric acid has likely diffused out slowly during soaking in PBS, thus leading to a weaker structure. This helps explaining the decrease of compressive strength with immersion time.

5 Conclusions

The present study showed that the obtained Mg- and Sr-substituted α-TCP cement pastes exhibited general good injectability characteristics even under a moderate maximum applied force of 100 N, which revealed to be dependent on the cement composition and on the LPR. Practically full injectable cement pastes were obtained for LPR $\geq$ 0.36 ml g^{-1}. The wet compressive strength of the hardened cements specimens is fairy high. Even the lower compressive strength values corresponding to the higher LPR used in the present work 0.38 ml g^{-1} are comparable to that of trabecular bone. These results shown that the brushite-forming α-TCP bone cements developed in the present work, especially the Sr-substituted one, hold an interesting promise for uses in trauma surgery such as for filling bone defects and in minimally invasive techniques such as percutaneous vertebroplasty to fill the lesions and to strengthen the osteoporotic bone.

Acknowledgments Thanks are due to CICECO for the support and to the Portuguese Foundation for Science and Technology for the fellowship grant of S. Pina (SFRH/BD/21761/2005). The first author is grateful to C. Stabler, from Institute of Mineralogie, University of Erlangen-Nuremberg, Germany, for his valuable help.

References

1. Gbureck U, Vorndran E, Muller FA, Barralet JE. Low temperature direct 3D printed bioceramics and biocomposites as drug release matrices. J Control Release. 2007;122:173–80.
2. Metallidis S, Topsis D, Nikolaidis J, Alexiadou E, Lazaraki G, Grovaris L, et al. Penetration of moxifloxacin and levofloxacin into cancellous and cortical bone in patients undergoing total hip arthroplasty. J Chemother. 2007;19:682–7.
3. Bohner M. Reactivity of calcium phosphate cements. J Mater Chem. 2007;17:3980–6.
4. Bohner M, Gbureck U, Barralet JE. Technological issues for the development of more efficient calcium phosphate bone cements: a critical assessment. Biomaterials. 2005;26:6423–9.
5. Fernandez E. Bioactive bone cements. Wiley Encyclopaedia of Biomedical Engineering. New York: Wiley; 2006.
6. Bohner M. Calcium orthophosphates in medicine: from ceramics to calcium phosphate cements. Inj-Intern Care Injur. 2000;31:37–47.
7. Dorozhkin SV. Calcium orthophosphates. J Mater Sci. 2007;42:1061–95.
8. Brown WE, Chow LC. A new calcium-phosphate setting cement. J Dent Res. 1983;62:672.
9. Wang XP, Ye JD, Wang H. Effects of additives on the rheological properties and injectability of a calcium phosphate bone substitute material. J Biomed Mater Res Appl Biomater. 2006;78:259–64.
10. Yuan HP, Li YB, de Bruijn JD, de Groot K, Zhang XD. Tissue responses of calcium phosphate cement: a study in dogs. Biomaterials. 2000;21:1283–90.
11. Alves HLR, dos Santos LA, Bergmann CP. Injectability evaluation of tricalcium phosphate bone cement. J Mater Sci Mater Med. 2008;19:2241–6.
12. Baroud G, Cayer E, Bohner M. Rheological characterization of concentrated aqueous á-tricalcium phosphate suspensions: the effect of liquid-to-powder ratio, milling time, and additives. Acta Biomater. 2005;1:357–63.
13. Boesel L, Reis RL. The effect of water uptake on the behaviour of hydrophilic cements in confined environments. Biomaterials. 2006;27:5627–33.
14. Bohner M, Baroud G. Injectability of calcium phosphate pastes. Biomaterials. 2005;26:1553–63.
15. Burguera EF, Xu HHK, Sun LM. Injectable calcium phosphate cement: effects of powder-to-liquid ratio and needle size. J Biomed Mater Res Appl Biomater. 2008;84:493–502.
16. Gauthier O, Muller R, von Stechow D, Lamy B, Weiss P, Bouler JM, et al. In vivo bone regeneration with injectable calcium phosphate biomaterial: a three-dimensional micro-computed tomographic, biomechanical and SEM study. Biomaterials. 2005;26:5444–53.
17. Baroud G, Wu JZ, Bohner M, Sponagel S, Steffen T. How to determine the permeability for cement infiltration of osteoporotic cancellous bone. Med Eng Phys. 2003;25:283–8.
18. Khairoun I, Boltong MG, Driessens FCM, Planell JA. Some factors controlling the injectability of calcium phosphate bone cements. J Mater Sci Mater Med. 1998;9:425–8.
19. Bai B, Jazrawi LM, Kummer FJ, Spivak JM. The use of an injectable, biodegradable calcium phosphate bone substitute for the prophylactic augmentation of osteoporotic vertebrae and the management of vertebral compression fractures. Spine. 1999;24:1521–6.
20. Ginebra MP, Rilliard A, Fernandez E, Elvira C, San Roman J, Planell JA. Mechanical and rheological improvement of a calcium phosphate cement by the addition of a polymeric drug. J Biomed Mater Res. 2001;57:113–8.
21. Sarda S, Fernandez E, Nilsson M, Balcells M, Planell JA. Kinetic study of citric acid influence on calcium phosphate bone cements as water-reducing agent. J Biomed Mater Res. 2002;61:653–9.
22. Gbureck U, Barralet JE, Spatz K, Grover LM, Thull R. Ionic modification of calcium phosphate cement viscosity. Part I: hypodermic injection and strength improvement of apatite cement. Biomaterials. 2004;25:2187–95.
23. Habib M, Baroud G, Gitzhofer F, Bohner M. Mechanisms underlying the limited injectability of hydraulic calcium phosphate paste. Acta Biomater. 2008;4:1465–71.
24. Barralet JE, Grover LM, Gbureck U. Ionic modification of calcium phosphate cement viscosity. Part II: hypodermic injection and strength improvement of brushite cement. Biomaterials. 2004;25:2197–203.
25. Sarda S, Fernandez E, Llorens J, Martinez S, Nilsson M, Planell JA. Rheological properties of an apatitic bone cement during initial setting. J Mater Sci Mater Med. 2001;12:905–9.
26. Leroux L, Hatim Z, Freche M, Lacout JL. Effects of various adjuvants (lactic acid, glycerol, and chitosan) on the injectability of a calcium phosphate cement. Bone. 1999;25:31–4.
27. Bigi A, Foresti E, Gandolfi M, Gazzano M, Roveri N. Isomorphous substitutions in beta-tricalcium phosphate: the different effects of zinc and strontium. J Inorg Biochem. 1997;66:259–65.
28. Kannan S, Lemos AF, Rocha JHG, Ferreira JMF. Characterization and mechanical performance of the Mg-stabilized á-Ca 3 (PO 4) 2 prepared from Mg-substituted Ca-deficient apatite. J Am Ceram Soc. 2006;89:2757–61.
29. Kannan S, Lemos IAF, Rocha JHG, Ferreira JMF. Synthesis and characterization of magnesium substituted biphasic mixtures of controlled hydroxyapatite/beta-tricalcium phosphate ratios. J Solid State Chem. 2005;178:3190–6.
30. Kannan S, Pina S, Ferreira JMF. Formation of strontium-stabilized á-tricalcium phosphate from calcium-deficient apatite. J Am Ceram Soc. 2006;89:3277–80.

31. Kannan S, Rocha JHG, Ferreira JMF. Synthesis and thermal stability of sodium, magnesium co-substituted hydroxyapatites. J Mater Chem. 2006;16:286–91.
32. Fadeev IV, Shvorneva LI, Barinov SM, Orlovskii VP. Synthesis and structure of magnesium-substituted hydroxyapatite 1. Inorg Mater. 2003;39:947–50.
33. Suchanek WL, Byrappa K, Shuk P, Riman RE, Janas VF, TenHuisen KS. Preparation of magnesium-substituted hydroxyapatite powders by the mechanochemical-hydrothermal method. Biomaterials. 2004;25:4647–57.
34. Lilley KJ, Gbureck U, Knowles JC, Farrar DF, Barralet JE. Cement from magnesium substituted hydroxyapatite. J Mater Sci Mater Med. 2005;16:455–60.
35. Rokita E, Hermes C, Nolting HF, Ryczek J. Substitution of calcium by strontium within selected calcium phosphates. J Cryst Growth. 1993;130:543–52.
36. Pina S, Olhero SM, Gheduzzi S, Miles AW, Ferreira JMF. Influence of setting liquid composition and liquid-to-powder ratio on properties of a Mg-substituted calcium phosphate cement. Acta Biomater. 2009;5:1233–40.
37. Mathew M, Schroeder LW, Dickens B, Brown WE. Crystal structure of alpha-$Ca_3(PO_4)_2$. Acta Crys: Struct Commun. 1977;33:1325–33.
38. Yashima M, Sakai A, Kamiyama T, Hoshikawa A. Crystal structure analysis of beta-tricalcium phosphate Ca-3(PO4)(2) by neutron powder diffraction. J Sol St Chem. 2003;175:272–7.
39. Curry NA, Jones DW. Crystal structure of brushite, calcium hydrogen orthophosphate dihydrate – neutron-diffraction investigation. J Chem Soc. 1971;23:3725–9.
40. Xu HHK, Weir MD, Burguera EF, Fraser AM. Injectable and macroporous calcium phosphate cement scaffold. Biomaterials. 2006;27:4279–87.
41. Lemos AF, Ferreira JMF. Combining foaming and starch consolidation methods to develop macroporous hydroxyapatite implants. Bioceram. 2004;254:1041–4.
42. Bohner M, Gbureck U. Thermal reactions of brushite cements. J Biomed Mater Res Appl Biomater. 2008;84:375–85.
43. Olhero SM, Ferreira JMF. Influence of particle size distribution on rheology and particle packing of silica-based suspensions. Powder Technol. 2004;139:69–75.
44. Mezger TG. The rheology handbook: for users of rotational and oscillation rheometers. Hannover: Vicentz Verlag; 2002.
45. Alkhralsat MH, Marino FT, Rodriguez CR, Jerez LB, Cabarcos EL. Combined effect of strontium and pyrophosphate on the properties of brushite cements. Acta Biomater. 2008;4:664–70.
46. TenHuisen KS, Brown PW. Effects of magnesium on the formation of calcium-deficient hydroxyapatite from $CaHPO_4{\cdot}2H_2O$ and $Ca_4(PO4)_2O$. J Biomed Mater Res. 1997;36:306–14.
47. Grynpas MD, Hamilton E, Cheung R, Tsouderos Y, Deloffre P, Hott M, et al. Strontium increases vertebral bone volume in rats at a low dose that does not induce detectable mineralization defect. Bone. 1996;18:253–9.
48. Saint-Jean SJ, Camire CL, Nevsten P, Hansen S, Ginebra MP. Study of the reactivity and in vitro bioactivity of Sr-substituted à-TCP cements. J Mater Sci Mater Med. 2005;16:993–1001.
49. Khairoun I, Driessens FCM, Boltong MG, Planell JA, Wenz R. Addition of cohesion promoters to calcium phosphate cements. Biomaterials. 1999;20:393–8.
50. Duck FA. Physical properties of tissue: a comprehensive reference book. London: Academic Press Limited; 1990.